Characterization of the vibrational dynamics in the octahedral sublattices of $LaD_{2.25}$ and $LaH_{2.25}$

1995 J. Phys.: Condens. Matter 7 7005

(http://iopscience.iop.org/0953-8984/7/35/007)

J. Phys.: Condens. Matter 7 (1995) 7005–7014. Printed in the UK

Characterization of the vibrational dynamics in the octahedral sublattices of $LaD_{2.25}$ and $LaH_{2.25}$

T J Udovic†, J J Rush† and I S Anderson‡

† Materials Science and Engineering Laboratory, National Institute of Standards and Technology, Gaithersburg, MD 20899, USA

‡ Institut Laue–Langevin, 38042 Grenoble Cédex, France

Received 3 April 1995, in final form 31 May 1995

Abstract. Incoherent inelastic neutron scattering spectroscopy was used to characterize the optic–vibrational density of states (DOS) of the octahedrally coordinated deuterium (D_o) and hydrogen (H_o) atoms in $LaD_{2.25}$, $LaH_{2.25}$, and $LaH_{2.03}$. The DOS exhibits a temperature- and concentration-dependent behaviour consistent with that observed previously for the analogous β-TbH_{2+x} system. At low temperature, the H_o DOS for $LaH_{2.03}$ is fairly sharp with minor spectral sidebands, indicating that the H_o atoms are predominantly isolated, with some atoms residing in short-range-ordered domains. Increasing the H_o (or D_o) concentration to $LaH_{2.25}$ (or $LaD_{2.25}$) yields a dispersion-broadened bimodal DOS characteristic of the H_o (or D_o) $I4/mmm$ long-range order that develops in the octahedral sublattice at low temperatures and these higher H_o (or D_o) concentrations. For $LaH_{2.25}$ at higher temperature (340 K), a broad, somewhat asymmetric DOS is suggestive of an H_o sublattice that is now largely disordered yet still possesses some degree of short-range order.

1. Introduction

Within the nominal fcc metal lattice structure of the superstoichiometric rare-earth dihydrides RH_{2+x} ($0 \leqslant x \leqslant x_{max} \leqslant 1$), hydrogen fully occupies the two tetrahedral interstices (t sites) per metal atom with the excess hydrogen x (below some maximum value, x_{max}) partially occupying the one octahedral interstice (o site) per metal atom. Recently, we determined by a neutron powder diffraction (NPD) study [1] that long-range ($I4/mmm$) ordering of the o site deuterium (D_o) atoms occurred at low temperature for the superstoichiometric light-rare-earth dideuteride $LaD_{2.25}$, accompanied by a tetragonal distortion of the metal lattice, an outward expansion of the cubic ensemble of eight t site deuterium (D_t) atoms surrounding each D_o atom, and a decrease in the c-axis-directed La–D_o bond distances by a displacement of the La atoms toward the D_o atoms (see figure 1(a)). Ideal order corresponded to full o site occupation for every fourth $(042)_C$ plane (where the subscript C refers to a cubic lattice basis) with all other $(042)_C$ planes empty. These results corroborated the ($I4/mmm$) ordering tendencies suggested by earlier NPD measurements of the related light-rare-earth compound $CeD_{2.26}$ [2] as well as the heavy-rare-earth compound TbD_{2+x} ($0.095 \leqslant x \leqslant 0.18$) [3]. More recent $TbD_{2.25}$ NPD data [4] for the D_o-ordered phase confirmed the presence of a slight tetragonal distortion and displacements of D_t and Tb atoms similar to those for the La and Ce deuterides, suggesting that the low-temperature $I4/mmm$ ordering and characteristic structural details displayed by these three rare-earth compounds are more or less common to other rare-earth deuterides for x near 0.25.

0953-8984/95/357005+10$19.50

In addition to the structural information provided by NPD, incoherent inelastic neutron scattering (IINS) has been shown [5] to be a sensitive vibrational probe of the H_o ordering in TbH_{2+x}. Specifically, the measured H_o optic–vibrational density of states (DOS) varied significantly with both H_o concentration x and temperature. For small x, the dilute H_o atoms were predominantly isolated in a local cubic environment and exhibited a sharp DOS that reflected the expected triply degenerate eigenstates. Increasing the H_o concentration at low temperature led to the onset and growth of the long-range ($I4/mmm$) order in the H_o sublattice [3, 4], accompanied by a transformation of the H_o DOS. At $x = 0.25$, each H_o atom possessed an identical local environment that was no longer cubic (see figure 1(b)), resulting in a bimodal H_o DOS, with each component broadened by lattice dynamics effects. By symmetry considerations, the doubly intense stiff mode was assigned to degenerate H_o vibrations in the identical a and b directions where the neighbouring o sites were occupied and the weaker soft mode was assigned to H_o vibrations along the c direction where the neighbouring o sites were vacant. Above the ordering temperature, this bimodal distribution reverted back to a DOS similar to that for small x, yet broadened by the persistence of some short-range order and/or the random occupation of o sites surrounding each H_o atom.

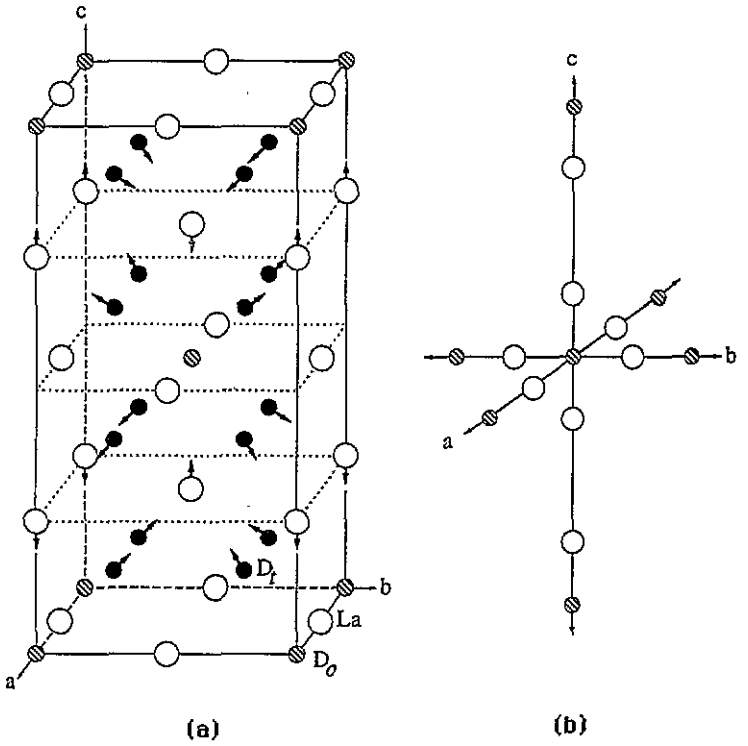

Figure 1. (a) Schematic diagram of the ($I4/mmm$) long-range-ordered $LaD_{2.25}$ structure and (b) the local environment surrounding each D_o atom in the three orthogonal directions.

A previous IINS study [6] suggested that the H_o DOS for $LaH_{2.1}$ possessed a temperature-dependent lineshape characterized by a broad singlet at 175 K transforming into a bimodal lineshape at 15 K. This change in lineshape was explained by a lowering of the H_o site symmetry at low temperature. The $LaH_{2.1}$ diffraction data indicated that, although the room-temperature data could be fitted with the cubic CaF_2 structure and the

H atoms on the high-symmetry sites, the 13 K data could only be fitted by allowing the H atoms to move along the [111] direction; the t site hydrogen (H_t) atoms were displaced only slightly while the H_o atoms were displaced by 0.137(9) Å. The splitting of the H_o DOS was justified by the fact that these off-centre H_o atoms would have two significantly different nearest-neighbour H_o–La distances.

Although the explanation forwarded above seemed reasonable, the $LaH_{2.1}$ data portrayed a strong resemblance to TbH_{2+x}. In light of the recent similar structural results for $LaD_{2.25}$ [1] and $TbD_{2.25}$ [4], it was clear that further temperature- and concentration-dependent vibrational spectroscopic data were necessary in order to clarify the true origin of the H_o splitting observed at low temperature. Hence, high-resolution IINS measurements of $LaD_{2.25}$, $LaH_{2.25}$, and $LaH_{2.03}$ were undertaken.

2. Experimental details

The $LaD_{2.25}$ sample was the identical one as used in the previous NPD study [1]. Synthesis of the La hydride samples followed the same procedure that was used to prepare the $LaD_{2.25}$ sample. Starting with ~27-g (for the deuteride) or ~10-g (for the hydrides) lots of high-purity La (99.99 at.%, Johnson–Matthey†), deuterium (Spectra Gases† research grade) or hydrogen (Matheson† research grade) were loaded by gas phase absorption in a quartz tube at 773 K to a nominal D(H)/La stoichiometry of 2.00. The samples were then allowed to equilibrate at 773 K for ~16–24 h followed by an 8–16 h evacuation to remove any excess o site D or H atoms, which are known to be unstable at this temperature [7], thus forming pure dideuteride or dihydride baseline compounds. The desired superstoichiometric compounds were made by adding additional deuterium or hydrogen to the baseline compounds at 773 K followed by a slow cooling to 503 K (685 K for $LaH_{2.03}$) and equilibrating there for ~6–15 h. Finally, the small deuterium or hydrogen vapour pressures above the samples were evacuated with a simultaneous rapid cooling to room temperature. The samples were transferred to a He-filled glove box, pulverized, and sealed in either a tubular V cell (for $LaD_{2.25}$) or thin-plate Al cells (for $LaH_{2.25}$ and $LaH_{2.03}$).

Neutron vibrational spectroscopic measurements were performed at the Neutron Beam Split-Core Reactor (NBSR) at the NIST using the BT-4 spectrometer with the high-resolution Be–graphite–Be–filter analyser and an assumed neutron final energy of 1.0 meV. Collimations of either 40′ or 20′ before and 20′ after the Cu(220) monochromator yielded instrumental energy resolutions (full width at half maximum, FWHM) depicted by the horizontal bars beneath the illustrated spectra. Lines through the spectra are intended only as guides to the eye.

3. Results and discussion

Figure 2 shows the H DOS for $LaH_{2.25}$ as a function of temperature. The H spectra are in general agreement with those reported for $LaH_{2.1}$ and display the expected DOS for H_o between 65 and 80 meV and H_t between 90 and 140 meV. Similar to the $LaH_{2.1}$ data, the H_o DOS for $LaH_{2.25}$ possesses a bimodal lineshape at low temperature which gradually disappears as the temperature is increased to 340 K. The two-peak H_t DOS, which is typical for the superstoichiometric rare-earth dihydrides [8], is a manifestation of H_o-H_t interactions [6, 8–10]. In general, for the ordered $RH_{2.25}$ structure, each H_t atom has one H_o nearest

† Manufacturers are identified in order to provide complete identification of experimental conditions and such identification is not intended as an endorsement by the NIST.

neighbour. The main 99 meV feature represents those H_t vibrations largely unperturbed by the presence of the H_o nearest neighbour, i.e., it is related to those vibrations polarized in the plane perpendicular to the H_o–H_t axis. In contrast, the high-energy 128 meV feature represents those vibrations polarized along the H_o–H_t axis and stiffened by the H_o–H_t interaction. This interaction clearly has a significant effect on the H_t DOS and has already been the subject of some discussion [6, 8–10]. The spectra in the present study are somewhat better-resolved than the $LaH_{2.1}$ spectra, more clearly delineating the structure in the spectral bands. Moreover, there are slight discrepancies in peak positions between the two studies, the H bands for $LaH_{2.1}$ estimated to be about 3-4% lower than the corresponding bands in the present study. The results of additional H_t DOS measurements for $LaH_{2.00}$ (not shown) located the scattering maximum at 102 meV compared with 99 meV for $LaH_{1.9}$ in the previous study [6], confirming this trend. Our $LaH_{2.00}$ value is more in line with that reported by Hunt and Ross [11] for $LaH_{1.92}$ at 103 meV. Since care was taken in the present study to ensure proper calibration of the instrument, this leads us to believe that there may have been a slight miscalibration of the energy transfer scale used in the previous study.

The low-temperature D DOS for $LaD_{2.25}$ is also depicted in figure 2, illustrating the analogous D_o band maximized at 53.3 meV and D_t bands at 71.5 and 92 meV. These bands are situated around 30% lower in energy than their H counterparts, as expected. Moreover, a well defined D_o 'overtone' band is evident at 106 meV, which corresponds with the more poorly defined H_o 'overtone' band for $LaH_{2.25}$ between 140 and 155 meV. The apparent higher clarity of the D_o 'overtone' band compared with its H_o counterpart stems mainly from better instrumental resolution and less attenuation from the Debye–Waller factor due to the relatively lower neutron momentum transfer involved. The D_o and H_o 'overtone' bands are approximately twice the energy of the fundamental o site bands and are evidence for the nearly harmonic nature of the o site potential.

It is interesting to compare the H_o/H_t peak area ratio ($r = A_o/A_t$) for our low-temperature $LaH_{2.25}$ spectrum with that for the $LaH_{2.1}$ data. Areas were determined after removing a linear baseline and excluding any scattering above 140 meV due to the H_o 'overtone' band. For $LaH_{2.25}$, $r = 0.124$, and for $LaH_{2.1}$, $r = 0.138$. This suggests that the H/La atom ratio for the '$LaH_{2.1}$' sample was underestimated. Assuming that our sample formula is correct, a premise supported by our previous $LaD_{2.25}$ structural study [1], we estimate that the '$LaH_{2.1}$' sample had the actual formula $LaH_{2.28}$. This is further corroborated by preliminary $LaH_{2.33}$ measurements (not shown) which indicate that the '$LaH_{2.1}$' spectrum fits qualitatively between the $LaH_{2.25}$ and $LaH_{2.33}$ spectra. The assumed $LaH_{2.28}$ formula places the H_o concentration of the '$LaH_{2.1}$' sample close to, yet actually above, that for our $LaH_{2.25}$ sample. This conclusion is also supported by '$LaH_{2.1}$' NPD data [6] which indicated an H_o/H_t atom ratio near 0.14, although the authors also report a somewhat lower value near 0.12 based on their IINS results. Of course, the authors assume that the overall H/La atom ratio is 2.1, and the larger-than-expected H_o concentration exists at the expense of a less-than-fully occupied t site sublattice. This assumption runs counter to the results of our $LaD_{2.25}$ NPD study [1], however, which indicate that the t site sublattice is essentially fully occupied at these temperatures. This discrepancy can be justified by the fact that the '$LaH_{2.1}$' samples were synthesized assuming that all La atoms in the starting metal were capable of participating in the hydriding process. It is well known now that this is not the case, the fraction of 'hydrideable' metal atoms being dependent on the starting metal purity [1, 12, 13]. Ignoring this fact often leads to the addition of too much hydrogen and larger-than-expected H/metal atom ratios, as was most likely the case for the '$LaH_{2.1}$' sample.

Figure 3 shows the higher-resolution H_o DOS for $LaH_{2.03}$ and $LaH_{2.25}$ and the D_o DOS

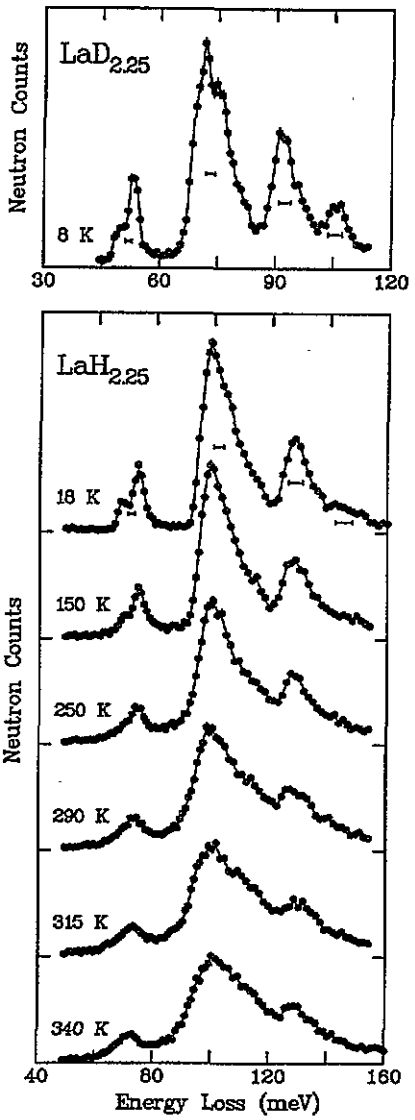

Figure 2. The temperature dependence of the H DOS for $LaH_{2.25}$ and the low-temperature D DOS for $LaD_{2.25}$.

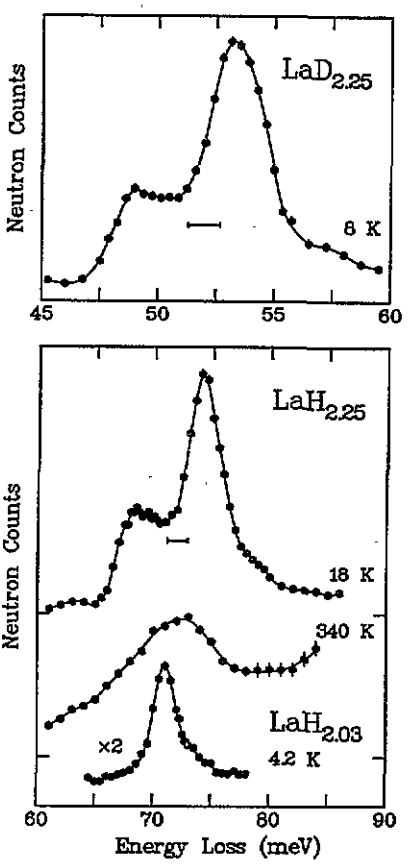

Figure 3. The H_o DOS for $LaH_{2.03}$ and $LaH_{2.25}$ and the D_o DOS for $LaD_{2.25}$.

for $LaD_{2.25}$. The concentration- and temperature-dependent behaviour of the spectra is reminiscent of that for TbH_{2+x} [5]. In particular, for $LaH_{2.03}$ (i.e., low H_o concentration) at low temperature, the H_o DOS feature at 70.9 meV is fairly sharp, indicating a predominance of isolated H_o atoms experiencing a locally cubic potential. In contrast, for $LaH_{2.25}$ (i.e., high H_o concentration) at low temperature, the H_o DOS possesses a dispersion-broadened bimodal lineshape with a 1:2 intensity ratio evident for the components of the spectral doublet located near 68.5 and 74.2 meV, respectively. An identical lineshape is also illustrated for the low-temperature D_o DOS of $LaD_{2.25}$ with analogous features located near

49 and 53.3 meV. As for $TbH_{2.25}$, it appears that the H_o DOS for $LaH_{2.25}$ is a reflection of the $I4/mmm$ order present at low temperature in the o site sublattice rather than a consequence of H_o atom displacement resulting in a lowering of site symmetry as suggested by the '$LaH_{2.1}$' study [6]. Again, symmetry and intensity considerations indicate that the low-energy component corresponds to H_o vibrations polarized along the c direction and the high-energy component corresponds to degenerate H_o vibrations polarized in the ab plane. The spectral splitting is presumably due to the presence of significant anisotropic H_o–H_o dynamic coupling interactions. The anisotropy results from the lower-than-cubic symmetry possessed by the ordered H_o sublattice. These conclusions are in agreement with recent first-principles calculations [14, 15] of H_o ordering in hypothetical β-$YH_{2.25}$, which suggested that the stability of the $I4/mmm$ structure is linked to the presence of relatively long-ranged interactions between H_o atoms, at least as far out as third-nearest-neighbour distances. Indeed, a preliminary IINS measurement [8] for $Tb(H_{0.1}D_{0.9})_{2.25}$ at low temperature indicates a collapse of the H_o DOS splitting, reflecting a breakdown in dynamic-coupling interactions that results from the isotope-dilution-induced isolation of H_o atoms from other H_o atoms. Moreover, no appreciable dynamic coupling can occur via the predominant H_o–D_o interactions present because of the large difference in H and D masses. Similar isotope-dilution-induced suppressions of H–H dynamic coupling interactions have also been spectroscopically observed in such systems as α-YH_x [16] and β-YH_2 [17].

Without similar isotope dilution measurements for $LaH_{2.25}$, we cannot unequivocally rule out the site-symmetry-lowering explanation for the splitting proposed in the '$LaH_{2.1}$' study [6], since one potential structural model in the recent $LaD_{2.25}$ NPD study [1] also suggested the possibility of similar D_o atom displacements in the $I4/mmm$-ordered state ~0.2 Å away from the high-symmetry positions. Yet, this explanation is not fully satisfactory for interpreting the observed H_o DOS spectrum for $LaH_{2.03}$. Such a spectrum would require a mixture of H_o atoms: some centred in high-symmetry positions and the rest shifted to low-symmetry positions. With respect to the isotope dilution measurements for $TbH_{2.25}$, one could argue, in addition, that the diluted H_o atoms in the predominantly deuterated $Tb(H_{0.1}D_{0.9})_{2.25}$ sample might not be participating in the long-range D_o ordering, and the apparent lack of H_o DOS splitting is an indication that these atoms are randomly occupying some of the remaining vacant o sites. Spectral interpretation of the observed H_o (singlet) and D_o (split) DOS would imply that all of the H_o atoms remain centred in high-symmetry positions whereas all of the D_o atoms are displaced to lower-symmetry positions. Although this possibility is hard to discount experimentally, we believe that such a distinct difference between H and D atom sitings portrays a physically unlikely situation. Thus, given the experimentally observed isostructural relationship between $TbH_{2.25}$ and $LaH_{2.25}$ and the suggested presence of long-ranged H_o–H_o interactions from first-principles calculations, we believe the facts strongly favour H_o–H_o interactions as the probable cause of the H_o DOS splitting for $LaH_{2.25}$ in the ordered state.

The previous $LaD_{2.25}$ NPD study [1] has determined that the D_o sublattice is almost completely disordered at 340 K. The 340 K spectrum in figure 3 illustrates the effect of this high-temperature disorder on the H_o DOS for $LaH_{2.25}$. The bimodal lineshape, which was prevalent at low-temperature, has now largely disappeared, being replaced by a considerably broader version of the low temperature H_o DOS for $LaH_{2.03}$. The spectrum is slightly compromised by the presence of some high-temperature-induced multiphonon scattering (which is absent at low temperature) on the low-energy side of the main scattering band. Nonetheless, the somewhat asymmetric lineshape suggests that some small degree of order still persists at this temperature. The NPD results at 340 K indicate that this order must be largely short ranged. The temperature dependence of the o site spectrum for $LaH_{2.25}$ is

consistent with that observed for $TbH_{2.19}$ [5] and $CeD_{2.12}$ [8].

It should be noted that the low-temperature H_o DOS peak for $LaH_{2.03}$, like that for $TbH_{2.03}$ [5], displays definite spectral sidebands, which are ascribed to the vibrations of 'nonisolated' H_o atoms, i.e., H_o atoms involved in o site sublattice domains of short-range order. The domain order is presumably similar to the long-range order which occurs at higher H_o concentrations, yet the domains for this low H_o concentration lack the size necessary to be detected by NPD measurements. For TbH_{2+x}, NPD data indicate that superlattice Bragg peaks due to long-range H_o order are absent for $x < 0.095$ [3] although electrical resistivity measurements of TbH_{2+x} [18] and various other RH_{2+x} systems [19–24] at low x values clearly support the contention that the H_o sublattice undergoes a disorder–order transformation upon cooling, as evidenced by a resistivity anomaly in the region of 150 to 200 K. Hence, even though NPD may be unable to detect the presence of short-range H_o order, it is apparent that the H_o DOS can indeed be used as a sensitive spectroscopic fingerprint of the H_o sublattice arrangement.

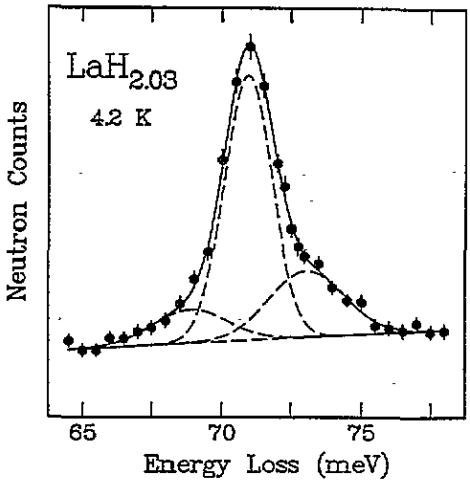

Figure 4. Three-component Gaussian fit (solid curve) of the high-resolution, low-temperature, H_o DOS for $LaH_{2.03}$. Component features are indicated by the dashed curves. The central peak represents the vibrations of isolated H_o atoms; the lower- and higher-energy sidebands represent vibrations of short-range-ordered H_o atoms along the c direction and in the ab plane, respectively. Details are described in the text.

In an effort to be more quantitative, a three-component Gaussian fit of the low-temperature H_o DOS for $LaH_{2.03}$ was performed. Table 1 summarizes the results. Initial fits which constrained the sidebands to have identical linewidths resulted in a nearly 1:2 intensity ratio for the lower- and higher-energy sidebands. In the final fit illustrated in figure 4, the lower- and higher-energy sidebands were additionally constrained to have a 1:2 intensity ratio. This fit is reasonable and locates the sidebands at 68.9 and 73.0 meV with widths of 3.1 meV FWHM and the central feature at 70.9 meV with a width of 2.0 meV FWHM. An attempt to constrain the sidebands to have equal intensities led to a slightly poorer fit with broader (4.0 meV FWHM) sidebands more closely situated at 70.3 and 72.7 meV and a narrower (1.8 meV FWHM) central feature located at 71.0 meV. Sidebands with equal intensities would be suggestive of a more basic H_o–H_o pairing phenomenon at this low H_o concentration (e.g., between H_o atoms occupying next-nearest-neighbour o sites along the a, b, and c directions), akin to what is spectroscopically observed for H_t–H_t pairing in some α-RH_x solid solutions [16, 25–28] and isolated D_t–D_t pairs in β-$Y(H_{0.9}D_{0.1})_2$ [17].

Table 1. The results of three-component Gaussian fits (with linear baselines) of the low-temperature H_o DOS for $LaH_{2.03}$. Subscripts 1, 2, and 3 refer to the central, lower-energy, and higher-energy components; E refers to the component position; W refers to the FWHM peakwidth; I refers to the integrated intensity normalized to a total three-component integrated intensity of 100; and χ_r refers to the reduced chi for the fit. Numbers in parentheses represent standard uncertainties in the last digits given.

Constraints	E_1 (meV) W_1 (meV) I_1	E_2 (meV) W_2 (meV) I_2	E_3 (meV) W_3 (meV) I_3	χ_r
$W_1 = W_2 = W_3$	70.98(3) 2.25(6) 77.5	68.4(3) 2.25(6) 7.1	73.5(1) 2.25(6) 15.4	0.783
$W_2 = W_3$	70.94(4) 2.0(2) 60.6	69.0(8) 3.2(8) 13.8	73.0(6) 3.2(8) 25.6	0.749
$W_2 = W_3$ $I_3 = 2I_2$	70.93(4) 2.0(1) 63.3	68.9(5) 3.1(7) 12.2	73.0(5) 3.1(7) 24.5	0.733
$W_2 = W_3$ $I_3 = I_2$	70.95(5) 1.8(1) 42.8	70.3(4) 4.0(9) 28.6	72.7(5) 4.0(9) 28.6	0.770

Yet, the theoretical [14, 15] and observed [1–4] stability of the $I4/mmm$-ordered structure in the RH_{2+x} systems at higher x values as well as the better fit using a 1:2 sideband intensity ratio favours the sideband lineshape that is similar to the low-temperature $LaH_{2.25}$ spectrum, representing H_o atoms located in short-range-ordered domains. The relative fitted intensities of the central and sideband features in figure 4 suggest that 63% of the H_o atoms are essentially isolated and the remaining 37% are involved in the short-range-ordered domains. This implies that low-temperature ordering tendencies are significant even at relatively low H_o concentrations.

The widths of the fitted features in figure 4 are somewhat larger than the 1.7 meV FWHM instrumental resolution. The larger widths of the sidebands probably reflect both the distribution of H_o local environments resulting from the finite-size effects of the domains and the presence of some phonon dispersion effects due to the ordered nature of the domains. Likewise, the slight broadness of the central feature also probably reflects a distribution of 'isolated' H_o local environments resulting from perturbations from more distant H_o neighbours, as well as possible vibrational contributions from 'nonisolated' H_o atoms located on the edges of the short-range-ordered domains.

It is useful to compare the fitted DOS for the 'nonisolated' H_o atoms comprising the short-range-ordered domains in $LaH_{2.03}$ with the low-temperature H_o DOS for $LaH_{2.25}$. Both spectra are superimposed in figure 5. The data indicate a smaller 4 meV splitting for the $LaH_{2.03}$ spectrum compared with the almost 6 meV splitting evident for the $LaH_{2.25}$ spectrum. This is consistent with the TbH_{2+x} results [5], which illustrate that the overall splitting appears to increase with increasing x. Moreover, the larger widths and more-complex lineshapes of the $LaH_{2.25}$ spectral components compared with those for $LaH_{2.03}$ are a reflection of more prominent lattice dynamics (i.e., dispersion) effects accompanying the presence of the long-range-ordered structure. Although the $LaH_{2.25}$ (as well as the $LaD_{2.25}$) spectrum could also be adequately fitted with multiple Gaussian components, no great effort was made at this time to characterize the spectrum more thoroughly, since elucidation of the

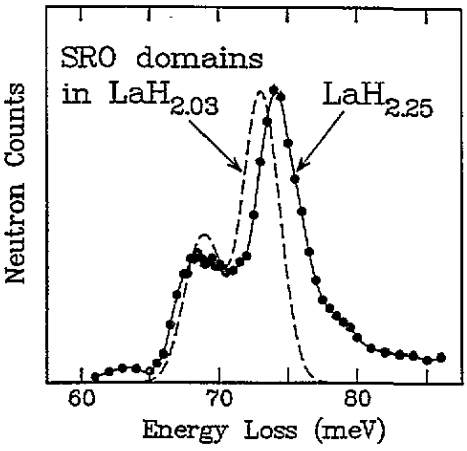

Figure 5. A comparison of the fitted H_o DOS for the short-range-ordered (SRO) domains in $LaH_{2.03}$ and the low-temperature H_o DOS for $LaH_{2.25}$.

spectral fine structure would involve detailed force field modelling of the lattice dynamics. The position of the $LaH_{2.03}$ spectrum, especially the high-energy feature, also appears to be downshifted by as much as 1 meV with respect to the $LaH_{2.25}$ spectrum. If this effect is real, it is certainly in line with the x-dependent behaviour of the LaH_{2+x} lattice constants, since it is typical for RH_{2+x} systems to undergo an overall lattice contraction with increasing x [29]. For $LaH_{2.03}$ at 4.2 K, which is believed to be cubic, we estimate the a_C (and c_C) lattice constant to be 5.661 Å [30]. For $LaH_{2.25}$ at 18 K, which is tetragonally distorted, we estimate a_T and $c_T/2$ to be 5.632 and 5.666 Å, respectively [30] (where the subscript T refers to a tetragonal lattice basis). Assuming that the short-range-ordered domains in $LaH_{2.03}$ remain locally undistorted means that the a_C lattice constant for the ordered domains in $LaH_{2.03}$ is ~0.5% larger than the a_T lattice constant for $LaH_{2.25}$, whereas the c_C lattice constant for the ordered domains in $LaH_{2.03}$ and the halved c_T lattice constant for $LaH_{2.25}$ are almost identical. Hence, as the fit suggests, larger lattice constants in the *ab* plane translate into weaker H_o–H_o interactions and correspondingly lower H_o vibrational energies in this plane, whereas similar lattice constants in the *c* direction translate into correspondingly similar H_o vibrational energies in this direction.

4. Summary

Incoherent inelastic neutron scattering spectroscopy was used to characterize the D and H optic–vibrational DOS in $LaD_{2.25}$, $LaH_{2.25}$, and $LaH_{2.03}$. The D_o and H_o DOS display a temperature- and concentration-dependent behaviour in line with that observed previously for β-TbH_{2+x}. In particular, for low-temperature $LaH_{2.03}$, the relatively sharp DOS indicates that the H_o atoms are largely isolated, with minor spectral sidebands suggesting that some of the H_o atoms become clustered in short-range-ordered domains. Increasing the H_o (or D_o) concentration to $LaH_{2.25}$ (or $LaD_{2.25}$) yields a dispersion-broadened bimodal DOS, similar to the previously reported '$LaH_{2.1}$' data, and characteristic of the H_o (or D_o) $I4/mmm$ long-range order that develops in the octahedral sublattice at low temperatures and these higher H_o (or D_o) concentrations. Raising the temperature of the $LaH_{2.25}$ to 340 K creates a broad, somewhat asymmetric DOS, which reflects a largely disordered H_o sublattice with some degree of lingering short-range correlations present among the H_o atoms. This study

illustrates the usefulness of the H_o DOS as a sensitive spectroscopic fingerprint of the details of the H_o sublattice arrangement, even in situations where the lack of long-range order hampers any structural characterization by neutron diffraction.

References

[1] Udovic T J, Huang Q, Rush J J, Schefer J and Anderson I S 1995 *Phys. Rev.* B **51** 12 116
[2] Fedotov V K, Fedotov V G, Kost M E and Ponyatovskii E G 1982 *Fiz. Tverd. Tela* **24** 2201 (Engl. Transl. *Sov. Phys.–Solid State*) **24** 1252
[3] André G, Blaschko O, Schwarz W, Daou J N and Vajda P 1992 *Phys. Rev.* B **46** 8644
[4] Huang Q, Udovic T J, Rush J J, Schefer J and Anderson I S 1995 *J. Alloys Compounds* at press
[5] Udovic T J, Rush J J and Anderson I S 1994 *Phys. Rev.* B **50** 7144
[6] Goldstone J A, Eckert J, Richards P M and Venturini E L 1986 *Physica* B **136** 183
[7] Vajda P, Daou J N and Burger J P 1987 *Phys. Rev.* B **36** 8669
[8] Udovic T J, Rush J J and Anderson I S 1995 *J. Alloys Compounds* at press
[9] Kamitakahara W A and Crawford R K 1982 *Solid State Commun.* **41** 843
[10] Vorderwisch P, Hautecler S and Lesmann T 1991 *J. Less-Common Met.* **172–174** 231
[11] Hunt D G and Ross D K 1976 *J. Less-Common Met.* **49** 169
[12] Daou J N, Lucasson A, Vajda P and Burger J P 1984 *J. Phys. F: Met. Phys.* **14** 2983
[13] Daou J N, Vajda P, Burger J P and Lucasson A 1986 *Phys. Status Solidi* a **98** 183
[14] Sun S N, Wang Y and Chou M Y 1994 *Phys. Rev.* B **49** 6481
[15] Wang Y and Chou M Y 1994 *Phys. Rev.* B **49** 10 731
[16] Anderson I S, Berk N F, Rush J J and Udovic T J 1988 *Phys. Rev.* B **37** 4358
[17] Udovic T J, Rush J J and Anderson I S 1994 *Phys. Rev.* B **50** 15739
[18] Vajda P, Daou J N, Burger J P and Lucasson A 1985 *Phys. Rev.* B **31** 6900
[19] Burger J P, Daou J N and Vajda P 1988 *Phil. Mag.* B **58** 349
[20] Vajda P, Daou J N and Burger J P 1991 *J. Less-Common Met.* **172–174** 271
[21] Daou J N and Vajda P 1992 *Phys. Rev.* B **45** 10 907
[22] Daou J N, Burger J P and Vajda P 1992 *Phil. Mag.* B **65** 127
[23] Vajda P and Daou J N 1993 *Z. Phys. Chem.* **179** 403
[24] Vajda P and Daou J N 1994 *Phys. Rev.* B **49** 3275
[25] Anderson I S, Rush J J, Udovic T and Rowe J M 1986 *Phys. Rev. Lett.* **57** 2822
[26] Udovic T J, Rush J J, Berk N F and Anderson I S 1992 *Phys. Rev.* B **45** 12 573
[27] Udovic T J, Rush J J, Berk N F, Anderson I S, Daou J N, Vajda P and Blaschko O 1993 *Z. Phys. Chem.* **179** 349
[28] Udovic T J, Rush J J, Anderson I S, Daou J N, Vajda P and Blaschko O 1994 *Phys. Rev.* B **50** 3696
[29] Chiheb M, Daou J N and Vajda P 1993 *Z. Phys. Chem.* **179** 255
[30] Boroch E, Condor K, Cai R-X and Kaldis E 1989 *J. Less-Common Met.* **156** 259